Materials Transactions, Vol. 46, No. 3 (2005) pp. 626 to 630

Experimental Investigation of Cavitation Behavior in AZ61 Magnesium Alloy

Juan Velázquez Aguirre*, Yorinobu Takigawa and Kenji Higashi

Department of Metallurgy and Materials Science, Osaka Prefecture University, Sakai 599-8531, Japan

The rate of cavitation with superplastic strain was investigated for a superplastic AZ61 magnesium alloy at a strain rate of $2 \times 10^{-4}\ s^{-1}$ and temperature of 648 K, under the conditions of which an elongation of more than 250% has been found. Cavities initiated at grain boundaries. The cavitation showed a growth perpendicular to the applied stress direction after the initial strains. The subsequent growth and coalescence of cavities invariably leads to failure of the material. The experimental growth rates are in good agreement with the rate predicted by the plasticity-controlled growth mechanism.

(Received October 15, 2004; Accepted January 31, 2005)

Keywords: *superplasticity, AZ61 magnesium alloy, cavitation, cavity growth rate*

1. Introduction

Recent research activities on magnesium materials have increased in an effort to reduce the weight of components in, for example, motor vehicles, for ecological reasons. This avenue is promising not only because of the relatively low density of magnesium, which can directly and substantially reduce vehicle weight, but also because of its good damping characteristics, dimensional stability, machinability, and low casting cost. These attributes enable magnesium to economically replace many zinc and aluminum die-castings, as well as cast iron and steel components.[1–15] However, in spite of these advantages, magnesium normally exhibits low ductility near and at room temperature because of its HCP structure. In order to exploit the benefits of magnesium materials, it is important to develop secondary processing, which can effectively produce complex engineering components directly from wrought products. Superplastic forming is a viable technique to fabricate hard-to-form materials into complex shapes.

The superplasticity refers to the ability of a crystalline material to exhibit large strains when pulled under tension. This phenomenon is of academic interest, but it also has considerable industrial potential, because it provides the capability for forming complex parts from materials. In general, the superplasticity is attained in the low strain rate range from 10^{-5} to $10^{-3}\ s^{-1}$ at relatively high temperatures of 0.8 T_m, where T_m is the absolute melting point of the material; 924 K for magnesium.[16] The superplastic strain rate range is rather low for commercial forming of structural materials, and the commercial viability of superplastic materials is therefore limited. Thus, one subject of interest is lowering the superplastic temperature or increasing the strain rate. Magnesium alloys, compared with aluminum alloys, which have a melting point similar to that of magnesium, have a high potential for superplasticity at lower temperature. This is because the pre-exponential factor for grain boundary diffusion, δD_{gb}, for magnesium is two orders of magnitude larger than that for aluminum, though their activation energies are nearly equivalent.[16] Low temperature superplastic behavior and low temperature superplastic forming have been investigated, and many kinds of magnesium alloys have been proposed. In the future, it is expected that magnesium alloys can be increasingly applied to create structural components, and it is therefore necessary to develop a secondary processing technique.

From a commercial point of view, the cavities are very important because they are likely to influence many post-forming properties of the alloys and to limit the range of applications of superplastically formed parts. Therefore, many studies of cavitation behavior in superplastic flow have been reported by using superplastic aluminum alloys;[17–29] however, the influence of the cavitation in this superplastic behavior has not yet been investigated and clarified by using superplastic magnesium alloys, though a limited study in AZ31 alloy[30] under GBS dominant deformation mechanism conditions has been reported. In this study, we examined the cavitation behavior by using the superplastic AZ61 magnesium alloy.

2. Experimental Procedures

The material used in this study was a commercial Mg-6 mass%Al-1 mass%Zn alloy (AZ61). The material was received as extruded in the form of a sheet with a thickness of 2.5 mm. The grain size, measured in previous research, was 17.1 μm.[3] The microstructure of the material is shown in Fig. 1; also, some observed precipitates are indicated. Observations made by the JEOL electron probe micro analyzer confirmed that these precipitates are composed of Mn and Al.

In previous research,[3] the present material demonstrated superplasticity at temperatures ranging from 523 to 673 K and at constant strain rates ranging from 10^{-6} to $10^{-3}\ s^{-1}$ in air with a strain rate sensitivity exponent (m) of 0.5, suggesting a grain boundary sliding (GBS) as the dominant deformation process. The variations in flow stress as a function of strain rate as well as the elongation observed at 648 K are shown in Fig. 2.

In order to carry out the metallographic investigation for the cavity formation, the specimens were tensile deformed normal to the extruded direction at a temperature of 648 K and a strain rate of $2 \times 10^{-4}\ s^{-1}$, under the conditions of which the activation energy has shown that the GBS

*Graduate Student, Osaka Prefecture University

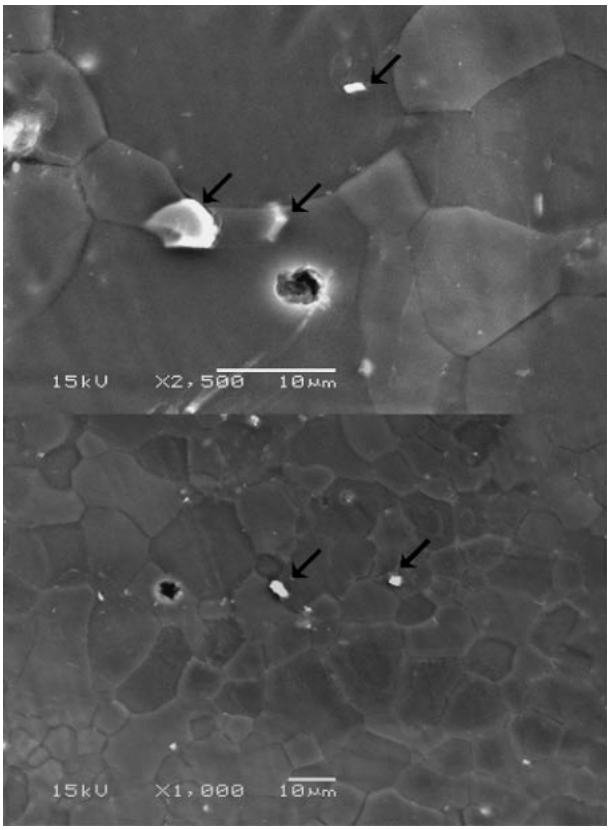

Fig. 1 Microstructure of AZ61 alloy showing equiaxed grains. Extrusion direction is horizontal. Some precipitates of Mn-Al (indicated by the arrows) and cavities with radius less than or equal to 1 μm are observed. Both precipitates and cavities are observed in the grain boundary.

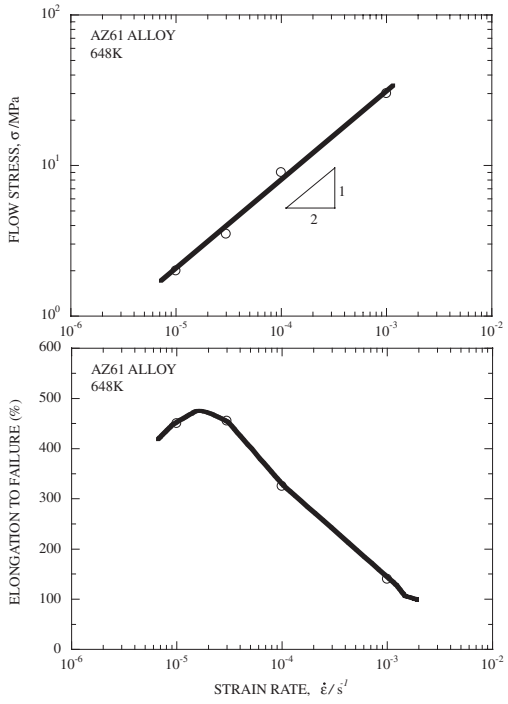

Fig. 2 The variation in flow stress and elongation to failure as a function of strain rate in AZ61.[3)]

mechanism is controlled by lattice diffusion. In addition, the specimens were cut in the deformed and un-deformed zones, then density measurements were made by pressure differentiation using the Shimadzu Micrometrics AccuPyc 1330. The volume of cavitation was assessed based on the difference in densities. The microstructural observations were made on the surface specimen after tensile tests were performed using scanning electron microscopy (SEM), which permitted measurements of cavity configurations to diameters as small as ≈0.3 μm. All cavities were assumed to be spherical for analysis of cavity size distribution. Finally, the data were analyzed to permit the construction of normalized plots showing the change in cavity morphology as a function of strain under these optimum testing conditions.

3. Results and Discussions

Figuer 3 shows scanning electron micrographs of the sample, a) non-deformed, and tensile tested at true strains of b) 0.41, c) 0.62, d) 0.71, e) 0.9, and f) 1.2. For the samples without deformation and strained at 0.9, cavities with maximum areas up to ≈3 μm^2 and ≈778 μm^2 (cavity radius ≈1 μm and ≈15.7 μm), respectively, were observed. Coalescence was observed at high strains, and appears to occur in a mixed intragranular mode.

Based on the SEM observations, the distributions of cavity diameters at strains of 0.2, 0.41, and 0.9 are shown in Fig. 4. As shown, with increasing strain the larger radius of cavities increases for the test conditions. The sizing interval was taken to be 1 μm. The total number of cavities increases with increasing strain, suggesting that continuous cavity nucleation is caused during the deformation. It was found that cavities of more than 9 μm in radius were very few and that the cavity radius where the maximum number was found was between 1 and 2 μm. The cavity diameters parallel (a) and perpendicular (b) to the tensile axis were measured; the relation b/a was observed around 1.4 from the initial 0.2 strain, suggesting that the cavitation growth occurs in a perpendicular direction.

3.1 Volume fraction of cavities

The evolution in terms of volume fraction of cavity with strain is shown in Fig. 5. Experiments in superplastic aluminum alloys had shown that the volume fraction of cavities increases exponentially with strain, suggesting that the void growth is essentially controlled by plasticity. The analysis predicted that the volume of cavities, C_v, should have an exponential dependence on strain, ε, according to the relation[19)]

$$C_v = V_0 \exp(\eta\varepsilon) \tag{1}$$

where V_0 is the volume of cavities at zero strain and η is the cavity growth rate parameter.

η is dependent on the material, strain rate, temperature, m value, and grain size, and it is in the range from 2 to 4 for many superplastic alloys.

The η parameter has been determined theoretically (for a single cavity) by the relation[19)]

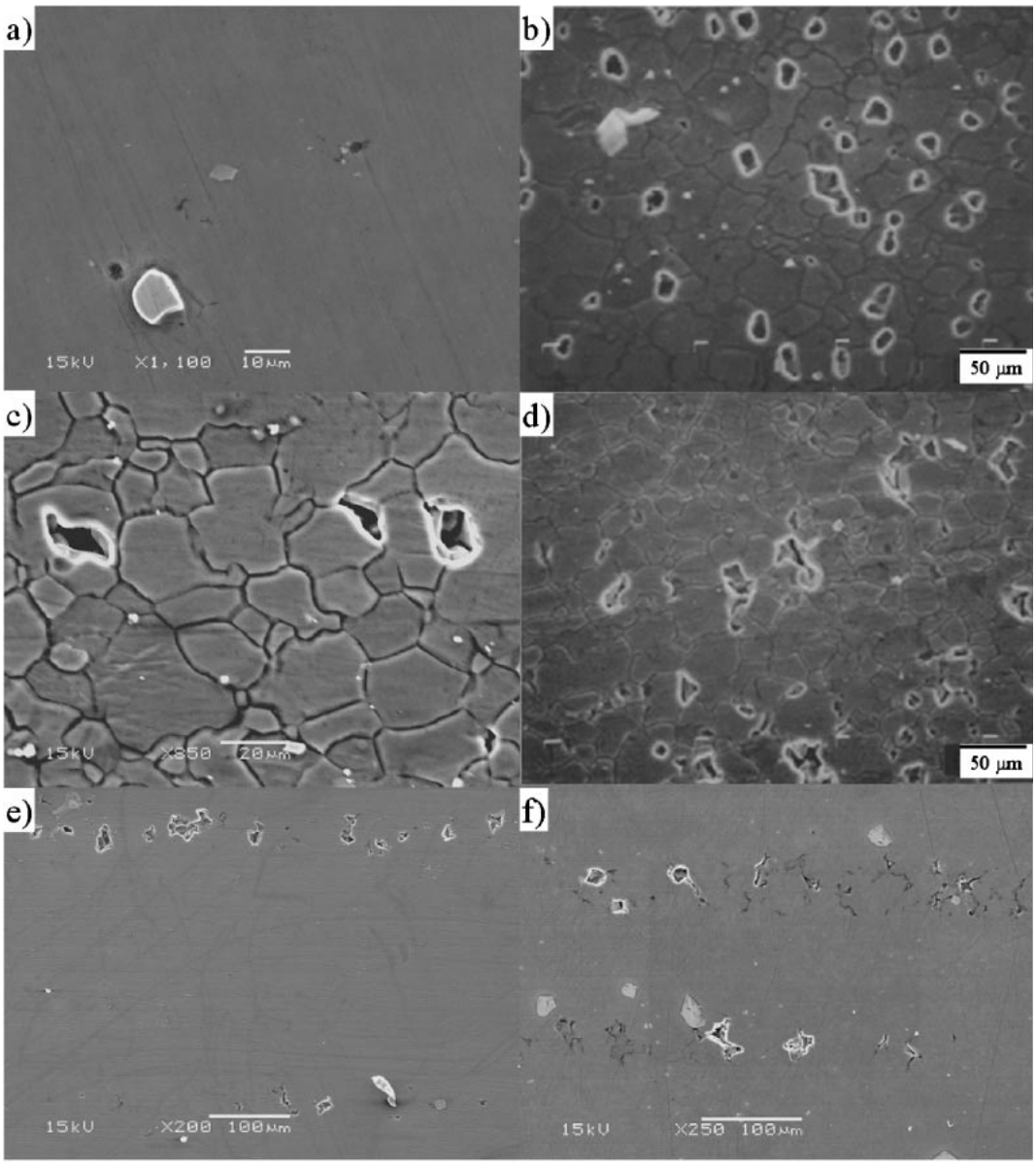

Fig. 3 Cavity morphology in the AZ61 alloy a) without deformation and strain at 648 K and a strain rate of $2 \times 10^{-4}\,s^{-1}$ to a predetermined true strain of b) 0.41, c) 0.62, d) 0.71, e) 0.9, and f) 1.2. The tensile direction is horizontal.

$$\eta = \frac{3}{2}\left(\frac{m+1}{m}\right)\sinh\left[2\left(\frac{2-m}{2+m}\right)\left(\frac{k_s}{3}\right)\right] \tag{2}$$

where k_s is a constant depending on the geometry of deformation and the extent of grain boundary sliding; $k_s = 1$ represents the case of no grain boundary sliding, and $k_s = 2$ that of freely sliding grain boundaries. For superplastic deformation, grain boundary sliding strain is approximated to be 50% of the accumulated strain,[22,31] leading to a value of 1.5 for k_s under optimum superplastic conditions; $\eta = 2.9$ for this experiment. The experimental $\eta = 2.8$, obtained from the slope of the relation shown in Fig. 5 and calculated from eq. (1), is in agreement with this value and with the superplastic behavior observed in previous research.[3]

3.2 Cavity growth rate

The cavity growth mechanisms for superplastic materials may be classified into three categories:[4,18,19,29] diffusion controlled, superplastic diffusion controlled, and plastic controlled.

When cavities grow by the diffusion of vacancies along the surrounding grain boundary, the rate of change of the cavity radius, r, with the total strain, ε, is given by

$$\frac{dr}{d\varepsilon} = \left(\frac{2\alpha\Omega\delta D_{GB}}{kT\dot{\varepsilon}r^2}\right)\left(\sigma - \frac{2\gamma}{r}\right) \tag{3}$$

Table 1 summarizes the constants to be used for the calculations.

As cavities grow, they become larger than the grain size, and vacancies diffuse into the cavities along many grain boundary paths. This process, known as superplastic diffusion growth, gives a growth rate in the form

$$\frac{dr}{d\varepsilon} = 45\,\frac{\Omega\delta D_{GB}\sigma}{kTd^2\dot{\varepsilon}} \tag{4}$$

The maximum radius measured in the material deformed at

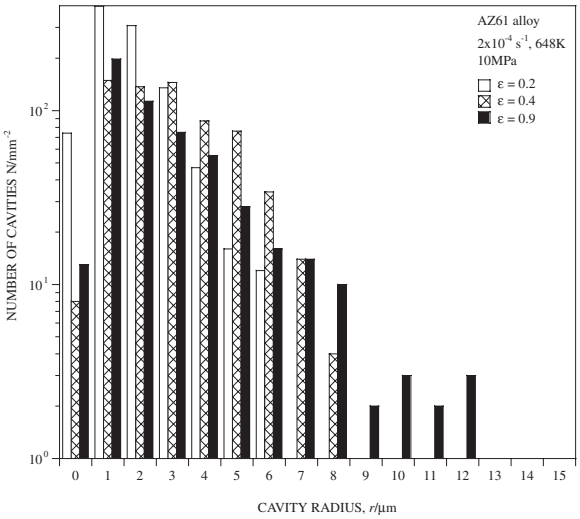

Fig. 4 Histogram showing the distribution of cavity diameters in the AZ61 alloy at strains of 0.2, 0.41, and 0.9.

0.9 strain was observed smaller than the grain size of the material indicating that under the experimental conditions superplastic growth mechanism was not present.

Alternatively, plasticity-controlled growth has a growth rate given by

$$\frac{dr}{d\varepsilon} = \frac{\eta}{3}\left(r - \frac{3\gamma}{2\sigma}\right) \tag{5}$$

The variation in cavity growth rate as a function of cavity radius calculated from eqs. (3) and (5) above are shown in Fig. 6. The experimental growth rates were calculated by the data of the 10 largest cavity radius and superimposed; these values were observed to be in agreement with the theoretically plastic growth controlled mechanism.

The average radiuses of the 10 biggest cavities measured from the cavity distribution as a function of strain are shown in Fig. 7. It can be seen that the cavity size increases with increasing strain, showing that cavity growth occurs during the deformation. Also, an exponential dependence of the

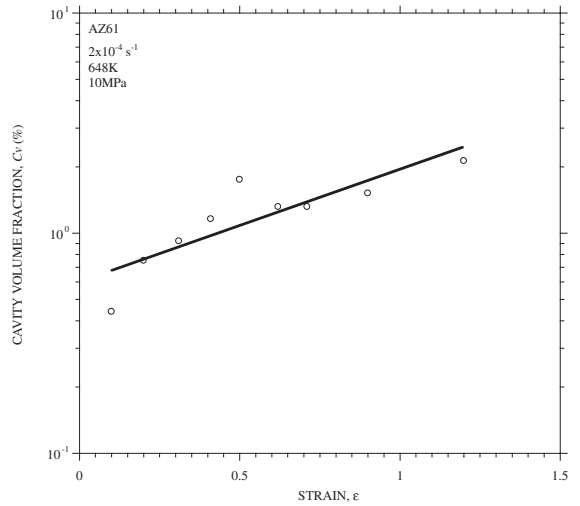

Fig. 5 The variation of volume of cavitation with strain at the test temperature of 648 K and strain rate of $2 \times 10^{-4}\,s^{-1}$ for the AZ61 alloy.

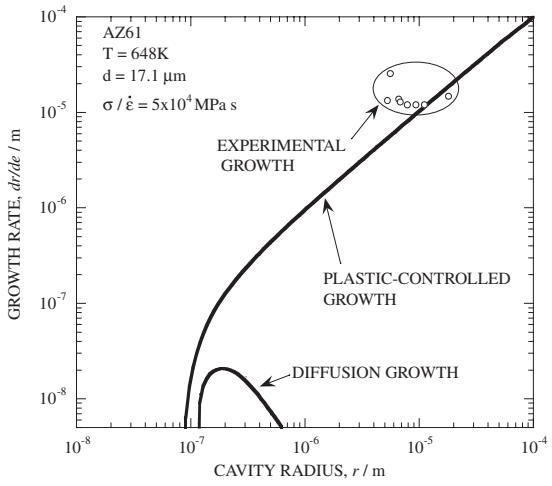

Fig. 6 The variation in cavity growth rate as a function of cavity radius for diffusion and plastic growth mechanisms for the AZ61 alloy. The experimental values from the 10 largest cavity sizes are indicated.

Table 1 Summary of testing conditions and values of constants used for calculations.

m	Strain rate sensitivity	0.5
α	Cavity size-spacing	1
Ω	Atomic volume (m^3)[a]	2.33×10^{-28}
D_{GB}	Grain boundary diffusion coefficient (m^3/s)[a]	$5 \times 10^{-12} \exp(-92000/RT)$
δ	Grain boundary width (m)	$2b$
b	Burgers vector (m)	3.2×10^{-10}
d	Grain size (m)	1.71×10^{-5}
T	Temperature (K)	648
σ	Stress (MPa)	10
$\dot{\varepsilon}$	Strain rate (s^{-1})	2×10^{-4}
γ	Surface energy (J/m^2)	0.56
R	Gas constant (J/mol K)	8.3
k	Boltzmann's constant (Nm/K)	1.38×10^{-23}

Data from[16)]

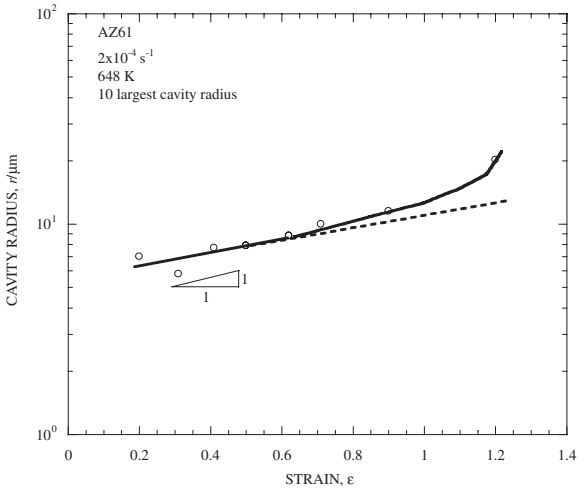

Fig. 7 Variation in cavity radius as a function of true strain for the AZ61 alloy calculated from eq. (8) and the experimental results. The cavity radius refers to the average radius of the 10 largest cavities.

cavity growth in low strains with a deviation at higher strains was observed from around 0.4∼0.5, perhaps for the appearance of coalescence observed in the cavity morphology shown in Fig. 3.

4. Conclusions

An AZ61 magnesium alloy exhibited a superplastic behavior with grain boundary sliding (GBS) dominant deformation process. Cavitation in the material without deformation was observed along the grain boundaries. The cavities are observed to initiate at the grain boundaries. Cavitation growth perpendicular to the applied stress direction was observed to result from the initial 0.2 strain. The experimental results showed that large cavities of more than 9 μm were few, and the cavity radius most frequently observed was between 1 and 2 μm. The experimental growth rates are in good agreement with the rate predicted by the plasticity-controlled growth mechanism.

Acknowledgments

This work was supported by the Light Metal Educational Foundation Inc.

REFERENCES

1) J. R. Davis: Magnesium and Magnesium Alloys, (Metals Handbook, Ohio, 1998) 559–574.
2) M. Mabuchi, K. Kubota and K. Higashi: Mater. Trans., JIM **36** (1995) 1249–1254.
3) H. Watanabe, T. Mukai, M. Kohzu, S. Watanabe and K. Higashi: Acta Mater. **47** (1999) 3753–3758.
4) T. G. Nieh, J. Wadsworth and O. D. Sherby: *Fine-structure superplastic metals: Magnesium based alloys*, (Superplasticity in Metals and Ceramics. Cambridge Solid State Series, 1997) pp. 69–73.
5) L. Gaines, R. Cuenca, F. Stodolsky and S. Wu: Automotive Technology Development. Detroit, Michigan (1996) pp. 24–28.
6) G. S. Cole: Mater. Sci. Forum. **419–422** (2003) 43–50.
7) H. Tsutsui, H. Watanabe, T. Mukai, M. Kohzu, S. Tanabe and K. Higashi: Mater. Trans., JIM **40** (1999) 931–934.
8) P. Mentenier, G. Gonzales-Doncel, O. R. Ruano, J. Wolfenstine and O. D. Sherby: Mater. Sci. Eng. **A125** (1990) 195–202.
9) M. Mabuchi, T. Asahina, H. Iwasaki and K. Higashi: Mater. Sci. Tech. **13** (1997) 825–831.
10) M. Mabuchi, K. Kubota and K. Higashi: Scr. Metall. Mater. **33** (1995) 331–335.
11) J. K. Soldberg, J. Tørklep, Ø. Bauger and H. Gjestland: Mater. Sci. Eng. **A134** (1991) 1201–1203.
12) H. Watanabe, T. Mukai, K. Ishikawa, Y. Okada, M. Kohzu and K. Higashi: J. Jpn. Inst. Light Metals. **49** (1999) 401–404.
13) H. Watanabe, T. Mukai, M. Mabuchi and K. Higashi: Scr. Mater. **41** (1999) 209–213.
14) H. Watanabe, T. Mukai, K. Ishikawa, M. Mabuchi and K. Higashi: Mater. Sci. Eng. **A307** (2001) 119–128.
15) H. Watanabe, T. Mukai, T. G. Nieh and K. Higashi: Scr. Mater. **42** (2000) 249–255.
16) H. J. Frost and M. F. Ashby: *Chapter 6: The Hexagonal Metals: Zn, Cd, Mg, and Ti*, (Deformation Mechanism Maps, Pergamon Press, Oxford, 1982) pp. 43–52.
17) H. Hosokawa, H. Iwasaki, T. Mori, M. Mabuchi, T. Tagata and K. Higashi: Acta Mater. **47** (1999) 1859–1867.
18) H. Iwasaki, T. Mori, M. Kodama, K. Higashi and S. Tanimura: Trans. Mat. Res. Soc. Jpn., **Vol. 14A** (1994) pp. 709–712.
19) J. Pilling and N. Ridley: *Cavitation and Fracture*, (Superplasticity in Crystalline Solid. The Institute of Metals. Ed. The Camelot Press. 1989) pp. 102–158.
20) D. H. Bae and A. K. Ghosh: Mater. Res. Soc. Symposium Procedure. **601** (2000) 61–66.
21) B. P. Kashyap and K. Tangri: Metall. Trans. A. **20A** (1989) 453–462.
22) D. H. Bae and A. K. Gosh: Acta Mater. **50** (2002) 993–1009.
23) J. Pilling, B. Geary and N. Ridley: Proc. Int. Cong. in Adv. Al and Mg Alloys. ASM Intl. (1991) pp. 823–828.
24) K. Higashi, T. G. Nieh and J. Wadsworth: Mater. Sci. Eng. **A188** (1994) 167–173.
25) H. Iwasaki, M. Takeuchi, T. Mori, M. Mabuchi and K. Higashi: Scr. Metall. Mater. **31** (1994) 255–260.
26) A. Varloteaux, J. J. Blandin and M. Suéry: Mater. Sci. Tech. **5** (1989) 1109–1117.
27) H. Iwasaki, T. Mori, M. Mabuchi and K. Higashi: Mater. Sci. Tech. **15** (1999) 180–184.
28) S. Wada, M. Mabuchi, K. Higashi and T. G. Langdon: J. Mater. Res. **11** (1996) 1755–1764.
29) A. H. Chokshi and T. G. Langdon: Acta Metall. **35** (1987) 1089–1101.
30) C. J. Lee and J. C. Huang: Acta Matell. **52** (2004) 3111–3122.
31) J. Pilling and N. Ridley: Acta Metall. **34** (1986) 669–679.